Photopolymerization of TiO2-based hybrid materials: effect of nanoparticles loading and photosensitive 1D microstructures fabrication

T T H Luu, Z. Jia, A. Kanaev, Luc Museur

Photopolymerization of TiO_2-based hybrid materials: Effect of nanoparticles loading and photosensitive 1D microstructures fabrication.

T.T.H. Luu [a], Z. Jia [a,b,c], A. Kanaev [b], L. Museur [a]*

a) Laboratoire de Physique des Lasers - LPL, CNRS UMR 7538, Université Paris 13, Sorbonne Paris Cité, 93430 Villetaneuse, France.

b) Laboratoire des Sciences des Procédés et des Matériaux - LSPM, CNRS, Université Paris 13, Sorbonne Paris Cité, 93430 Villetaneuse, France.

c) Dalian Research Institute of Petroleum and Petrochemicals, SINOPEC, Dalian 116045, China;

Keywords : organic-inorganic hybrids, composites, polymer, photopolymerization, TiO_2 nanoparticles, microstructure, photosensitivity.

Corresponding Author

* luc.museur@univ-paris13.fr

00 33 1 49 40 37 24

ABSTRACT

Hybrid materials, based on inorganic nanoblocks incorporated into polymer networks, are an important class of functional materials. Although the kinetic of the free-radical polymerization of neat polymers has been studied for many years, both theoretically and experimentally, studies devoted to the polymerization kinetics of nanocomposite materials are rare. In this study, photosensitive hybrids formed using poly(2-hydroxyethyl methacrylate) (pHEMA) and titanium dioxide (TiO_2) nanoparticles functionalized with polymerizable ligands were considered. Their bulk UV-induced free-radical photopolymerization was investigated to evaluate the potential of pHEMA/TiO_2 hybrids as a material of choice for the fabrication of micro-optical devices. The influence of the nanoparticle concentration and UV intensity on the polymerization kinetics, probed in situ by Raman spectroscopy, is discussed. A decrease in the initiation rate was observed, which was attributed to the UV absorption of TiO_2 nanoparticles. This leads to a decrease in the propagation rate with an increase in nanoparticle concentration. Furthermore, a decrease in the maximum C=C conversion yield was observed when the nanoparticle concentration was increased. This was attributed to the formation of microgel regions around the nanoparticles, which prevented the polymer chains from bonding with surface ligands. Despite the lower conversion yield, we demonstrated the fabrication of one dimension (1D) photoactive microstructures in pHEMA/TiO_2 hybrids. The photochromic efficiency of the obtained structure was evaluated based on the reduction of silver (Ag) ions under UV irradiation. The results show that pHEMA/TiO_2 hybrids can be considered as a prospective material for the realization of photosensitive microelements.

1. INTRODUCTION

The broad interest in organic-inorganic hybrid materials over the past two decades has been motivated by the possibility of combining the useful properties of their two constituent components [1, 2]. Many studies have been conducted to control the synthesis of these nanocomposite materials and understand their physical properties [3]. Soft chemistry is one of the most widely used approaches for preparing and incorporating inorganic building blocks into organic polymer matrices [4]. The mechanical, thermal, and physical properties of the obtained nanocomposites were improved compared with those of the neat polymer. These materials can also acquire new properties directly related to the nature of the interactions at the interface between organic and inorganic components [5]. Currently, these hybrids are used in a wide range of fields including optics, electronics, optoelectronics, protective coatings, sensors, and solar cells, etc. [2, 6]. Hybrids based on silica, titania, and zirconia have attracted particular interest because of their high refractive index and biocompatibility [7-9]. Despite evident achievements, in situ polymerization in the presence of functionalized inorganic blocks such as nanoparticles (NPs) has not yet been well documented and understood. Although the kinetics of the free radical polymerization (FRP) of neat polymers have been studied for many years, both theoretically and experimentally [10, 11], only few studies have been devoted to the polymerization kinetics of polymers combined with nanoparticles. It appears that the presence of inorganic nanoparticles significantly modifies the FRP kinetics. Compared to a solution of neat monomers, acceleration or retardation of polymerization reactions has been reported depending on the nature of the ligands functionalized on the nanoparticle surface [12-19]. Moreover, the influence of NPs on initiator decomposition and chain transfer reactions to the monomer must be considered Due to a large diversity of side reactions that can be possibly induced in presence of nanoparticles, theoretical models considering their influence on polymerization kinetics are very rare. Verros et al. proposed a model based on mass balance equations to describe the radical polymerization of methyl methacrylate (MMA) in presence of different kinds of non

polymerizable nano-additives [20]. In this work, diffusional limitations on initiation, propagation and termination reactions have been taken into account using appropriate equations based on free volume theory. In addition to the possible effect of nano-additives on both free volume fraction and glass transition temperature of the reaction mixture, the authors underlined the role of nano-additives as radical scavengers, causing deactivation of macroradicals and primary initiator radicals.

Hybrid materials, which combine mechanical and optical properties of their organic and inorganic components, have found numerous applications in optics and photonics [6, 21, 22]. We have previously reported the preparation of hybrids containing preformed monodispersed titanium oxo-alkoxy (TOA) nanoparticles embedded in organic poly(2-hydroxethyl methacrylate) (pHEMA) matrix [23-28]. In situ polymerization was induced either by the thermal activation of an initiator [23-25], or by the use of high pressures in the absence of an initiator [27-30]. In addition to the increase in refractive index compared to neat pHEMA, these hybrids have also shown reversible photochromic [23, 31] and photorefractive properties [32], making them good candidates for applications in integrated optics. Some of these applications, such as fabrication of micro-optic element like gratings, couplers, waveguides or 3D photonic structures, require precise shaping of the material on micro- or sub-micrometric scales [22]. Free radical photopolymerization, triggered by absorption of one or two photons, became then a method of choice because it allows the spatial control of polymerization reactions on the sub-micrometric scale [33, 34]. However, in order to ensure a good mechanical stability of the obtained structures, only multifunctional monomers, leading to an important crosslinking between polymeric chains, are usually considered in this connection. This issue is even more critical in the case of hybrid materials, in which inorganic component strongly affects polymerization of the organic phase. Therefore, a detailed understanding of the effects of titania nanoparticles on the reactions and processes involved in photopolymerization of HEMA is required before considering the realization of micro-optical components based on pHEMA/TiO_2 nanoparticulate hybrids.

In this study, we analyzed the effect of TiO_2 nanoparticles concentration and light intensity on the bulk free-radical photopolymerization of HEMA/TiO_2 hybrid solutions under UV irradiation. The polymerization reactions were probed in situ by Raman spectroscopy. Conversely, to the most commonly used experimental methods, based on differential scanning calorimetry (DSC) or dilatometry, which are indirect and can have response times too long to properly monitor in situ fast polymerization reactions, spectroscopic approaches, such as Raman spectroscopies, allow the evolution of the reaction to be monitored by direct observation of the disappearance of the C=C double bonds in monomers. Polymerization reactions occurring in a fraction of a second can thus be studied. With this approach, influence of TiO_2 nanoparticles insertion can be clarified not only on the final conversion yield of HEMA monomers but also on the polymerization kinetics of the hybrid solutions. To test the potential of pHEMA/TiO_2 hybrids in the fabrication of microptical components, 1D micrometric structures were realized using interference lithography and their photoactivity was demonstrated.

2. Experimental section

2.1. Materials

Liquid HEMA (purity >99%) was purchased from Sigma-Aldrich. Before use, oxygen was removed by repeated freeze–thaw cycles. The liquid HEMA was frozen using liquid nitrogen and pumped under vacuum for a few minutes until freezing. Phenylbis(2,4,6-trimethylbenzoyl)phosphine oxide (BAPO, 97%) was purchased from Sigma-Aldrich and used as a photoinitiator without further purification. It was mixed with HEMA at concentration 0.5 wt% under a controlled atmosphere.

For the fabrication of 1D microstructures, 3-(acryloyloxy)-2-hydroxypropyl methacrylate (AHPMA), purchased from Sigma Aldrich, was used as a crosslinker. The mixture was then mixed with the HEMA-TiO_2 hybrid solution, without further purification. Acetyl acetone, used as a development agent for 1D microstructures, was purchased from Sigma-Aldrich.

2.2. Hybrids synthesis

The pHEMA-TiO_2 hybrids were prepared as previously described by Gorbovyi et al. [23]. Briefly, size-selected titanium-oxo-alkoxo (TOA) nanoparticles with a diameter of 5 nm were generated in a thermostatic sol-gel reactor with rapid micromixing using a titanium tetraisopropoxyde (TTIP) precursor (Acros Organics, 98% purity) and distilled water in a 2-propanol (Acros Organics, 99.5% purity) solution and a hydrolysis ratio H=2.0 at 20.0 °C. Through a one-step hydrolysis-condensation transformation, the underlying sol-gel chemistry results in well-defined titanium-oxo-alkoxo $TiO_{2-(x+y)}/2(O^iPr)_x(OH)_y$ nanoparticles composed of a metal oxide core with surface propoxy (O^iPr) and hydroxy (OH) groups. Under the applied experimental conditions, the obtained nanocolloids were almost monodispersed and stable beyond one day [35], which allowed their relatively simple manipulation. In the second step, the TOA colloids in 2-propanol were mixed with HEMA, and solvent exchange (2-propanol by HEMA) was carried out overnight under vacuum (~1 mbar), leading to 2-propanol solvent removal and replacement of $–O^iPr$ ligands by –OEMA (the deprotonated form of HEMA) at the nanoparticle surface without changes in the nanoparticle size. At this stage the concentration of the inorganic component in the hybrids solution could be increased from 0.15 mol/l in the original colloid up to 3.0 mol/l in the hydrid solution. The TOA/HEMA hybrid solutions with varying titania content used in this study are listed in Table 1.

In the final step, the hybrid solutions were placed under a controlled atmosphere between two glass plates separated by 250 µm using a 1 × 1 cm adhesive gene frame (Thermo Scientific). This procedure prevented continuous diffusion of atmospheric oxygen through the sample during the laser irradiation experiments. A high-repetition-rate (10 kHz) UV laser delivering pulses of 7 ns at 355 nm and mean power of 10 mW (CNI MPL-F-355) was used to photopolymerize the hybrid solutions. The laser beam was expanded to irradiate the entire surface of the sample and its power was controlled using a set of polarizers (Figure S1.a).

Sample name	Volume of nanoparticles suspension mixed with 5 ml of HEMA (ml)	HEMA : Ti molar ratio	C_{Ti}, mol/l
X5	25	11 : 1	0.75
X10	50	5.5 : 1	1.5
X20	100	2.7 : 1	3

Table 1: pHEMA-TiO_2 hybrid samples composition (see text for details)

Thin films were prepared for the fabrication of 1D microstructures. An HEMA-TiO_2 hybrid solution containing a crosslinker (AHPMA) was deposited on the surface of a clean glass plate. Thin films of 10 μm thickness were then prepared using a spin coater device at a speed of 1000 rpm for 20s. The entire process was performed under yellow light. After preparation, the thin films were stored in a black box to avoid any interaction with external light.

2.3. Experimental methods.

The kinetics of photopolymerization under UV irradiation was studied by Raman spectroscopy. All Raman spectra of the samples were measured at room temperature in a backscattering configuration using an HR800 spectrometer equipped with a Peltier-cooled CCD detector (Horiba Jobin Yvon) with spectral and spatial resolutions of 0.25 cm^{-1} and 5 μm, respectively. In-situ Raman measurements were performed by focusing the probe beam at 640 nm in the middle of the sample.

The FRP process was monitored by a decrease in the intensity of the C=C bond stretching band at 1640 cm^{-1} of the HEMA monomer, which was simultaneously accompanied by an increase in the intensity of the C-CH_2 band (1455 cm^{-1}). The spectra were normalized to the intensity of the C=O band at 1730 cm^{-1}, which is not involved in the polymerization process (Figure S1.b). After fitting the Raman spectra with a multi-peak function, the conversion yield (CY) of the monomer was calculated as [28]

$$CY(t) = 1 - \frac{\left(I_{C=C} / I_{C=O}\right)_t}{\left(I_{C=C} / I_{C=O}\right)_{t=0}} \quad (1)$$

where $I_{C=C}$ and $I_{C=O}$ are the areas of ν(C=C) and ν(C=O) Raman bands before irradiation (*t=0*) and at irradiation time *t*. To calculate the rate of polymerization, $CY(t)$ was first smoothed using the rlowess algorithm. The normalized rate of polymerization was then obtained directly from the smoothed conversion yield, as follows:

$$R_p = \frac{d\,CY}{dt} \quad (2)$$

To monitor the FRP reaction in real time, the Raman spectra were recorded every 0.5s during the total process duration of typically 500 s. Each series of measurements was repeated at least four times to ensure good reproducibility. The data presented in this article are based on the average of these measurements.

To realize 1D microstructures, we used a simple direct laser writing approach, in which the original hybrid solutions were exposed to interference patterns formed by the superposition of two UV beams. The aforementioned UV laser (CNI MPL-F-355) was used for this purpose. The main laser beam, with a diameter of 5 mm, was divided into two subbeams using a beam splitter. The optical paths of both beams were adjusted using mirrors to ensure the same path length through the optical system before the beams interfered with the sample surface.

3. RESULTS AND DISCUSSION

Under UV irradiation, BAPO dissociates to form phosphinoyl and benzoyl primary radicals, which react with monomers to initiate polymerization. Figures 1 and 2 show the conversion yields and polymerization rates of pristine HEMA and hybrids with different NP concentrations under UV irradiation at intensities of 1 and 0.1 mW/cm^2. In the case of HEMA, the maximum conversion yield (approximately 80%) did not depend on UV intensity. In addition, we clearly observed an auto-

acceleration of the reaction characterized by an increase of the rate of polymerization (R_p), which is a typical feature of FRP process [36]. A large number of more or less sophisticated models describing this effect can be find in literature (see for example recent reviews [11, 37]). These works attribute the auto-acceleration effect to the gradual diffusion-control of propagation and termination reactions as the polymerization reaction proceeds and the reaction mixture becomes increasingly dense. Indeed, in the early process stage, the rates of initiation (R_i) and termination (R_T) reactions are equal, resulting in a constant rate of propagation (R_p). As polymerization progresses, the viscosity increases because of the higher concentration of macromolecules. The movement of macroradicals to meet and react together is significantly impeded. As a result, the rate of termination decreases and the concentration of macroradicals increases, leading to an increase in the propagation rate up to the maximum value $R_{p,max}$. At higher conversion yields, progressive vitrification of the medium occurs, reducing the monomer mobility, leading to a decrease in the polymerization rate, and eventually to the stop of the reaction. A higher UV intensity has the effect of an apparent acceleration of the process, in the sense that the maximum conversion yield is reached earlier. The effect of UV light intensity on the photopolymerization kinetics of HEMA has recently been investigated in more detail [38].

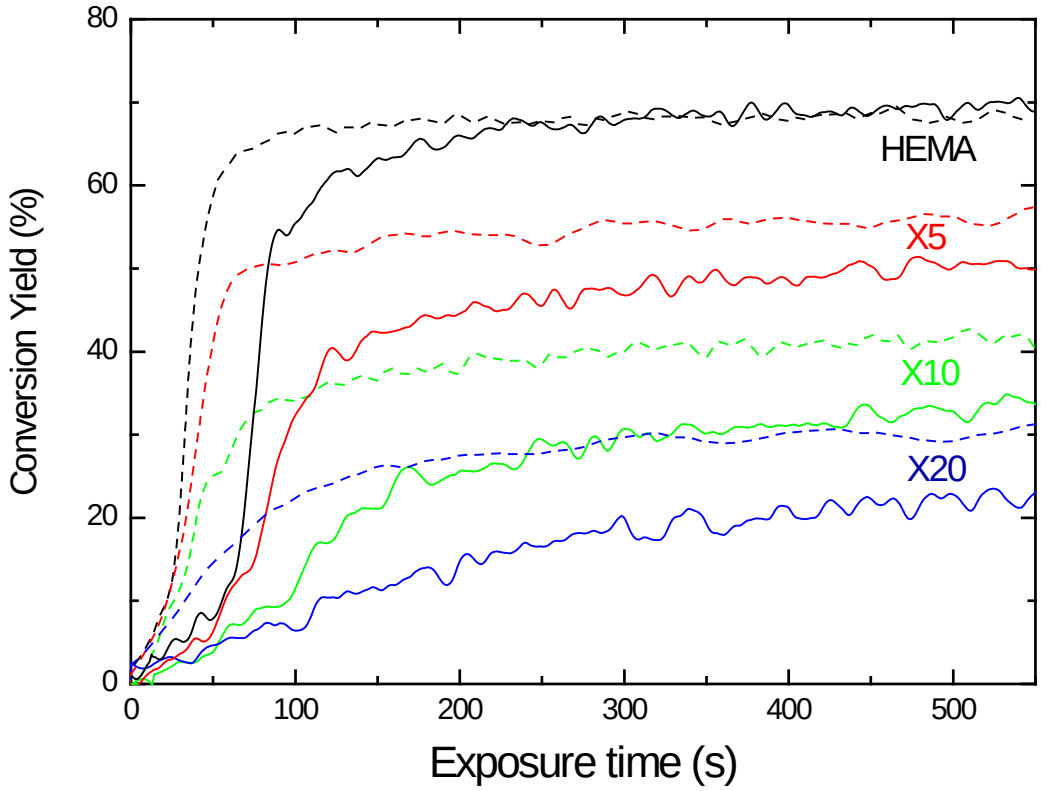

Figure 1: Conversion yield of C=C double bond measured in HEMA and hybrids under UV irradiation with 1 mW/cm^2 (- -) and 0.1 mW/cm^2 (—) UV-laser intensities.

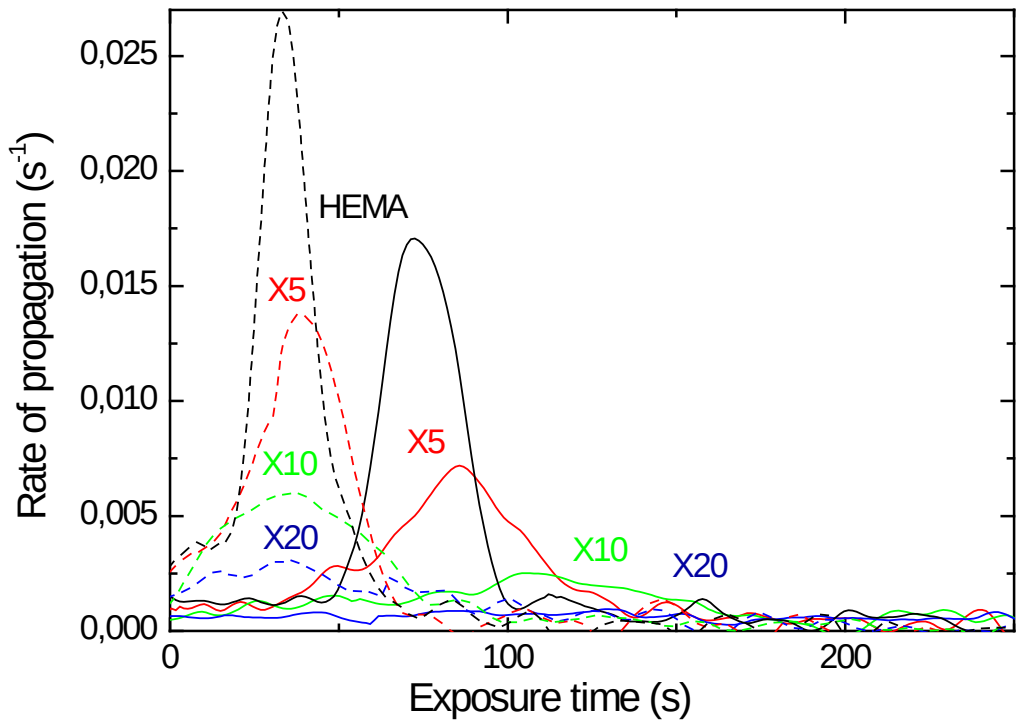

Figure 2: Propagation rate in HEMA and hybrids under UV irradiation with 1 mW/cm^2 (- -) and 0.1 mW/cm^2 (—) UV-laser intensities.

The kinetics of the photopolymerization reaction changed both when titania nanoparticles were mixed with HEMA and UV light intensity was increased. Regarding first the effects of UV intensity. As in the case of pure HEMA a higher UV intensity has led to an acceleration of the polymerization process. However, contrary to what has been observed in neat HEMA, a higher UV intensity, and consequently a higher rate of initiation, results in a higher maximum conversion yield at the end of the reaction. Thus, a minimum of 22% was obtained for sample X20 irradiated with 0.1 mW/cm^2, while with an intensity of 1 mW/cm^2 about 30% of the monomers are converted (Figure 1). In fact, the formation of a polymer network is accompanied by volume shrinkage, which rate is much slower than that of the propagation reaction. The temporary excess of free volume thus induced, maintains the mobility of monomers and radicals, which promotes their reactions leading to higher conversion yields than those obtained under equilibrium conditions.

The effects of nanoparticles contents on polymerization kinetics are manifold. First of all, as can be seen of Figure 1, the higher the titania concentration, the lower is the maximum conversion yield. Moreover, the autoacceleration effect seems to be less pronounced when the titanium oxide concentration increases, until it no longer occurs in the X20 sample. This last point is more clearly evidenced by the evolution of propagation rates, as shown in Figure 2. Indeed, the maximum rate faded, and eventually disappeared, when the titania concentration increased. A third consequence of nanoparticle loading can be observed. Indeed, the presence of NPs appeared to slow the reaction, since the maximum propagation rate was observed later. This is particularly visible at low UV intensities (Figure 2). As mentioned above, NPs functionalized with polymerizable OEMA ligands are expected to copolymerize with free HEMA monomers. Radical polymerization between the OEMA ligands is also expected to occur on the nanoparticle surface. The observed slowing of the reaction as the nanoparticle concentration increases is therefore surprising, since the addition of multifunctional monomers to a solution of monofunctional monomers is expected to advance the gelation process [10, 39]. Actually, it appears that the functionalized titania NP's affect both the initiation and propagation rates. The reasons for these changes are discussed below.

We first analyse the effect of nanoparticles concentration on the initiation rate and show that the observed decrease is not related to the deactivation of macro or primary radicals initiator as usually proposed in literature. At the very beginning of the polymerization process, steady-state conditions are fulfilled, and the propagation reaction rate can be expressed as

$$\frac{dCY}{dt} = k_{p0}(1-CY)\left(\frac{R_i}{2\,k_{t0}}\right)^{0.5} \text{ with } R_i = 2\,f\,\sigma_{PI}\,[PI]\,I_{L/2} \quad (1)$$

where f is the initiator efficiency, $\sigma_{PI} = 2.9\ 10^{-18}\ cm^2$ is the photoinitiator absorption cross section, and $I_{L/2}$ is the incident UV light intensity at the point where Raman analysis is performed. Assuming that the photoinitiator concentration [PI] and the initial rate constants of propagation (k_{p0}) and termination (k_{t0}) do not vary, the integration of Equation (1) yields

$$-\ln(1-CY) = k_{eff}\,t \quad \text{with} \quad k_{eff} = k_{p0}\left(\frac{R_i}{2k_{t0}}\right)^{0.5} \quad (2)$$

The linear fit of $\ln(1-CY)$ as a function of time allowed us to obtain the overall rate constant k_{eff} for different concentrations of titania nanoparticles. These values are plotted in Figure 3. a), where a decrease in k_{eff} is observed with increasing TiO_2 content. As one can see, the overall rate constant is higher at 1 mW/cm^2 than at 0.1 mW/cm^2. According to Equation (2), this difference corresponds to the square root of the ratio of initiation rates, $k_{eff,\,1mW/cm^2} / k_{eff,\,0.1mW/cm^2} = \sqrt{R_{i,\,1mW/cm^2} / R_{i,\,0.1mW/cm^2}} = \sqrt{10}$, as indicated by the dotted line in Figure 3. a). Because it is unlikely that k_{p0} and k_{t0} change in the presence of TiO_2, these experiments reflect a decrease in the initiation rate with an increase in titania NP concentration.

The reason of this decrease is the following. In the synthesis of nanocomposites based on the in situ polymerization of acrylates or methacrylate monomers, the reduction in the initiation rate with inorganic content is usually attributed to the influence on primary radicals of the hydroxyl groups present on the NP surface [17-19, 40]. It has been suggested that primary radicals undergo chain transfer by H abstraction to the hydroxyl groups, thus forming oxygen radicals on the surface.

These newly formed radicals can then scavenge another radical and/or be involved in termination reactions, which lead to a reduction in radical efficiency and result in a slowdown of the reaction. However, this mechanism may be not effective in the present experiment. Indeed, the observed decrease in the initiation rate seems to be mainly related to the UV absorption of the titania nanoparticles. Figure 3.b) shows the evolution of the effective rate constant ratio, $k_{eff}(hybrid)/k_{eff}(HEMA)$, for different samples at two UV laser intensities. This ratio can be easily calculated by considering that the UV intensity in the middle of the sample is expressed as $I_{L/2} = I_0 \exp\left(-\left(\sigma_{TiO_2}[TiO_2] + \sigma_{PI}[PI]\right)L/2\right)$, where I_0 is the incident UV light intensity, and $\sigma_{TiO_2} = 4.3\,10^{-20}\,cm^2$ [23] is the absorption cross-section of TiO_2 at 355 nm. The calculated ratio, represented by the dashed line in Figure 3.b), is in good agreement with the measurements. Thus, OEMA ligands grafted onto the titania surface probably prevent the interaction of primary radicals with surface hydroxyl groups. This interpretation is in agreement with results recently reported by Lin *et al*. who analysed the FRP of MMA in presence of SiO_2 nanoparticles [17]. They observed that when the SiO2 surface is grafted with ligands bearing reactive double bonds, the grafted polymer layer generated in situ, effectively prevents initiator molecules and free radicals from being wasted by reacting with the surface hydroxyl groups. Finally, we can consider that the primary radicals have a constant initiator efficiency, which can be estimated from the k_{eff} values of the HEMA solution. Using the rate constants $k_{p0} = 10^3\,M^{-1}s^{-1}$ and $k_{t0} = 1.1\,10^6\,M^{-1}s^{-1}$ found in the literature [41], we obtained an average value of $f = 0.4$, which is consistent with the reported value of BAPO quantum yield of photodissociation under UV irradiation $\phi = 0.6$ [42].

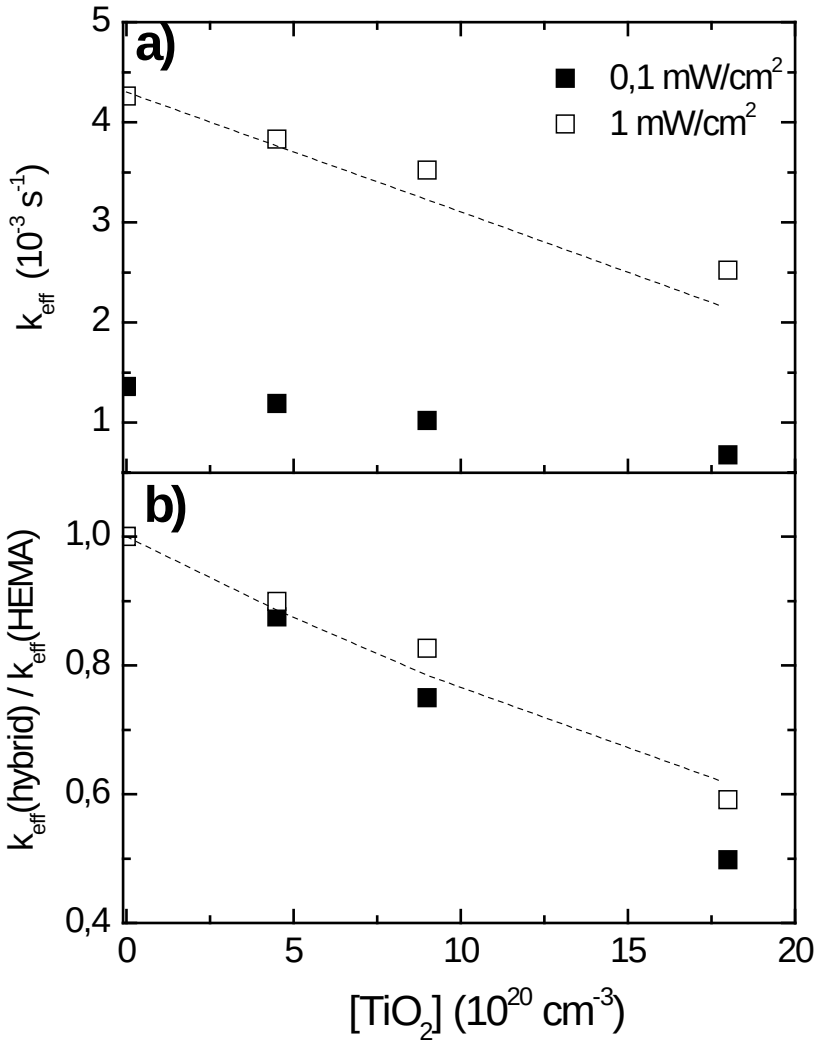

Figure 3 : **(a)** Overall rate constant k_{eff} measured for different concentrations of titania nanoparticles in hybrids and UV intensities 0.1 mW/cm^2 (■) and 1 mW/cm^2 (□). The dashed line represents $\sqrt{10}\ k_{eff,\,0.1mW/cm^2}$ **. (b)** Evolution of measured effective rate constants ratio $k_{eff}(TiO_2)/k_{eff}(HEMA)$ for different concentrations of titania nanoparticles and UV intensities 0.1 mW/cm^2 (■) and 1 mW/cm^2 (□).The dashed line represents the calculated ratio taking into account UV absorption of titania nanoparticles (see text for details).

We now discuss the influence of titania NP on the auto-acceleration process of polymerization reaction. In their analysis of in situ bulk polymerization of MMA in presence of zinc oxide (ZnO) nanoparticles, Demir *et al*. [18] observed the suppression of the auto-acceleration effect when ZnO NP are added to MMA solution. They assigned this effect to a degenerative chain-transfer reaction of macroradicals induced by hydroxyl groups present on nanoparticles surface. Since in our

system, OEMA ligands grafted on TiO_2 nanoparticles appear to prevent interactions with surface hydroxyl groups, we do not consider this interpretation. Actually, at long processing times, steady-state conditions could no longer be verified. However, the propagation rate is still directly related to the concentration of radical polymer chains. The observed autoacceleration (Figure.2) was due to an increase in the concentration of these macroradicals as a result of the progressive hindrance of their translational movement when the polymer network grew. The disappearance of the autoacceleration effect when the TiO_2 NPs concentration was increased may be related to the heterogeneity of the reaction medium. Indeed, hybrid polymerization involves two distinct populations of radicals with strongly different reactivity: on the one hand, free radical polymer chains in the bulk, which polymerize as in pure HEMA, and on the other hand, radicals localized on OEMA groups grafted on titania nanoparticles. These latter are immobilized on the nanoparticle surface and, therefore, have a lower reactivity than free macroradicals. Under these conditions, the propagation rate can be written as [15]

$$R_{p-Hybrid} = k_{p-HEMA}[M]\left[R^{\bullet}\right]_{HEMA} + k_{p-OEMA}[M]\left[R^{\bullet}\right]_{OEMA} \quad \text{with } k_{p-OEMA} \ll k_{p-HEMA}$$

where k_{p-HEMA} and k_{p-OEMA} are the propagation rate constants of the radicals localized on the free HEMA polymer chains and OEMA ligands, respectively, and $\left[R^{\bullet}\right]_{HEMA}$ and $\left[R^{\bullet}\right]_{OEMA}$ corresponding radicals concentrations. Thus, the rate of polymerization in the hybrids was always lower than that of pure HEMA. Moreover, only free macroradicals, whose movement is significantly affected by the growth of the polymer structure, are involved in autoacceleration phenomena. Thus, as their concentration decreased with increasing titanium content, auto-acceleration was less pronounced, and eventually the polymerization rate became constant, as shown in Figure 2, for the samples with the highest titania concentration.

The third observed effect of the nanoparticle loading was a reduction in the maximum conversion yield measured at the end of the polymerization process (Figure 1). Achilias et al. [16] studied the in situ bulk polymerization of HEMA in the presence of different types of nano-additives.

They observed a reduction in the maximum conversion yield when the surface groups of the nano-additives promoted the formation of hydrogen bonds with the monomers. In the present study, the polymerizable nature of the ligands influenced the final conversion yield. Indeed, along the reaction, the grafted nanoparticles were incorporated into the growing polymer chains as particular units containing a large number of pendant double bonds. Propagation proceeds further through the addition of monomers from a radical site on the OEMA ligand. This process can lead to cross-linking if another nanoparticle is incorporated in the growing polymer chain or to a type of cyclization reaction when one of the remaining pendant double bonds of the same nanoparticle reacts with the propagating macroradical. If realized, this can result in the formation of microgel regions, inside which many unreacted pendant double bonds and monomers are entrapped. The reactivity of these species then decreases because their access by radicals is gradually prevented by the development of a polymer network. Because of this shielding effect, as well as the drop in radical mobility in the course of the reactions, many of these unreacted double bonds will never react, thus limiting the final conversion yield with respect to HEMA polymerization. This effect was more pronounced when the titania nanoparticle concentration increased.

It is worth noting that spatial inhomogeneities introduced by the formation of microgel regions may be responsible for the reduction in the mechanical strength of hybrids with high nanoparticle content. Indeed, hybrids with titania concentrations higher than 4M are brittle and can be easily reduced to powder when pressed between two fingers. The use of high pressure allows to overcome this limitation and to synthetize hybrids with titania concentrations as high as 12M [27].

The results presented above indicate that increasing the concentration of TiO_2 nanoparticles decreases the maximum conversion rate of the C=C double bonds, which affects the mechanical stability of the hybrid material. On the other hand, the refraction and photochromic response of the material are enhanced with an increase in the nanoparticle concentration [23, 32]. For these hybrids to be used in the fabrication of optical microelements, the polymerization effectiveness and photoactivity of the realized microstructures must be tested. This issue was addressed in the last part

of this study. To fabricate the microstructures, the original hybrid solutions were exposed to the interference pattern formed by the superposition of two UV laser beams. In neat pHEMA, entanglement of the polymer chains and hydrogen bonds plays an important role in the cohesion of the polymer network. Indeed, all OH groups on the pHEMA side chain are thought to be involved in OH…OH or OH…O=C type of hydrogen bonds [43, 44]. However, the addition of nano additives can strongly affect the formation of H- bonds [16], which reduce the stability of the polymer network, particularly when the size of the polymerized volume is reduced. Our results show that the addition of a cross-linking agent is necessary to achieve the formation of stable solid microstructures in pHEMA/TiO_2 hybrids. This could be directly related to the formation of the microgel regions discussed above, and indicates that if functionalized TiO_2 nanoparticles act as cross-linkers, they seem to only contribute to the formation of very loose networks. Finally, 1D stable structures were obtained by adding AHPMA (38 vol%) as a crosslinker agent to the HEMA-TiO_2 hybrid solutions. Figure 4 shows the structure of the X10 hybrids after irradiation at a UV intensity of 7 mW/cm^2 for 7 s. A parallel linear stripe relief of ~2 µm in height and regularly spaced by 10 µm, covering a surface area of a few mm^2, was observed after the development procedure.

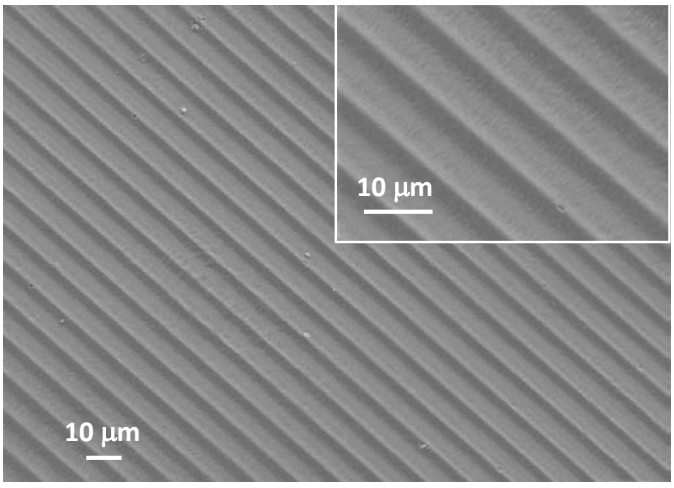

Figure 4 : 1D structures of X10 hybrids obtained under UV-laser irradiation (intensity 7 mW/cm^2, irradiation time 7s).

Finally, we verified that the development procedure of former 1D microstructures did not modify the hybrid composition by removing the titanium dioxide nanoparticles, and preserve the photosensitivity of the hybrids. The photoactivity of pHEMA/TiO_2 hybrids is related to an efficient separation and trapping of photoinduced charges at the organic/inorganic interface under UV irradiation [23, 26]. As a consequence of the trapping of photoinduced electrons as small polarons Ti^{3+}, the photocatalytic reduction of Ag^+ ions on the surface of titanium oxo-alkoxy nanoparticles has been previously reported [45]. This effect was used to evaluate the photosensitivity of the fabricated microstructures. Following the procedure proposed in [45], the X10 hybrid microstructure was immersed in an aqueous solution of $AgNO_3$ and illuminated at a UV intensity of 38 mW/cm^2 for 300 s. Energy dispersive X–ray spectroscopy (EDX) analysis was performed to confirm the formation of Ag particles by the reduction of Ag^+ ions on the surface (Figure 5). While only the lines assigned to C (0.277 keV), O (0.523 keV), and Ti (0.452 and 4.508 keV) were observed in the fresh sample, the presence of Ag (2.984 keV) was observed after UV light illumination. More evidence is presented in the inset of Figure 5, which shows an SEM image of the surface of the UV-light-treated sample. The observed nanoparticles covering the surface were assigned to reduced silver. The optical absorption measurements shown in Figure 6 support this conclusion. The higher absorption observed on the sample after treatment can be assigned to the Ag plasmon absorption of core-shell Ag&TiO_2 nanoparticles with a small Ag shell thickness of D_{sh}≤0.5 nm around titania nanoparticles of 5 nm in diameter (see inset in Figure 6). This is an expected result considering the short deposition time [45] and easy penetration of silver ions into the polymer-like material.

These results show that pHEMA/TIO_2 hybrids can be considered as materials of interest for the realization of photosensitive microstructures. Optimization of the hybrid solution composition is in progress by our group with the aim of increasing the TiO_2 nanoparticle concentration without losing mechanical stability and realizing photoactive and high-refractive-index structures with submicronic spatial resolution.

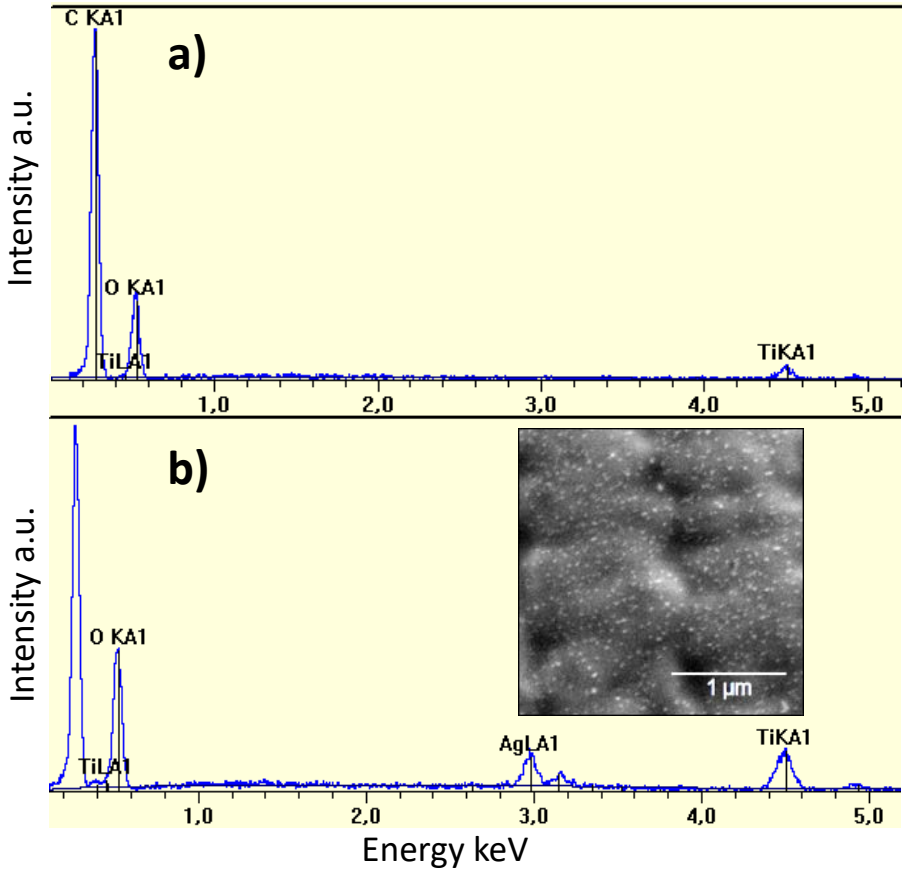

Figure 5: Energy dispersive X–ray measurement before (a) and after (b) Ag^+ ions reduction on microstructured X10 hybrid sample. SEM image of sample surface covered with Ag nanoparticles is shown in insert

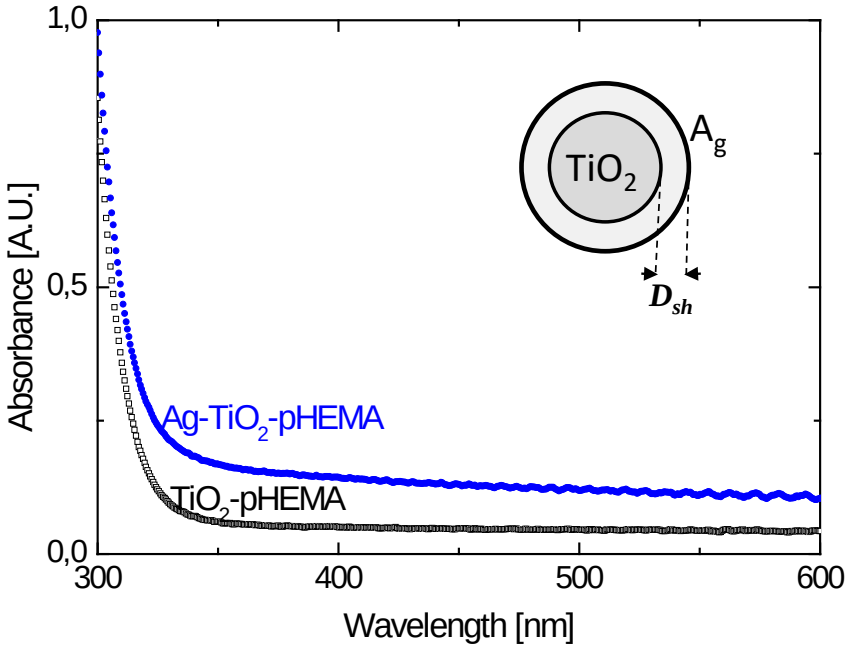

Figure 6 : Absorption spectra of microstructured X10 hybrid sample before (black) and after (blue) the Ag^+ ion reduction. The insert shows a scheme of the core shell $Ag@TiO_2$ nanoparticles responsible of the absorption in the visible range.

4. CONCLUSION AND PROSPECTS

In this study, we investigated the bulk free-radical UV photopolymerization of original hybrid materials formed from two components: organic HEMA and inorganic TiO_2 nanoparticles functionalized with polymerizable ligands. The influence of the nanoparticle concentration on the kinetics of the polymerization reaction was studied using Raman spectroscopy. We showed that a decrease in the initiation rate resulted from the absorption of UV photons by the nanoparticles, and not from the loss of efficiency of primary radicals due to chemical reactions with the surface ligands. This effect explains the pronounced decrease in propagation rate with increasing nanoparticle concentration. Furthermore, we assigned a decrease in the conversion yield of the C=C double bond with an increase in TiO_2 loading to the formation of microgel regions around the nanoparticles, which prevented polymerization of the surface ligands.

The fabrication of 1D microstructures was demonstrated using direct UV laser writing. The photochromic efficiency of the obtained structure was evaluated based on the reduction of Ag^+ ions under UV irradiation. Our results show that pHEMA/TiO_2 hybrids can be considered as prospective key materials for the realization of photosensitive microoptical elements.

The results of this study contribute to the development and applications of organic-inorganic hybrid nanocomposites obtained by in situ free radical polymerization. Moreover, they may also provide an experimental basis for further development of theoretical models devoted to the polymerization of organic/inorganic hybrid materials. Indeed, since side reactions induced the presence of functionalized TiO_2 nanoparticles in an HEMA solution are less numerous than in other hybrids systems involving nanoadditives, these hybrid solutions may serve as a model system to address these issues.

ACKNOLEDGMENTS

Andrey B. Evlyukhin is acknowledged for fruitful discussions regarding the interpretation of the absorption spectra of Ag, and Ag&TiO_2 nanoparticles.

ANR (Agence Nationale de la Recherche) and CGI (Commissariat à l'Investissement d'Avenir) are gratefully acknowledged for their financial support of this work through the Labex SEAM (Science and Engineering for Advanced Materials and devices) ANR 11 LABX 086, ANR 11 IDEX 05 02. The Federative Structure IFR "Paris Nord Plaine de France" in Materials Science is gratefully acknowledged.

CREDIT AUTHOR STATEMENT

T.T.H. Luu: Investigation, formal analysis, data curation, visualization, and validation. **Z. Jia**: Investigation, data curation, visualization, validation, writing review, and editing. **A. Kanaev**: Conceptualization, writing review, and editing. **L. Museur:** Conceptualization, funding acquisition, supervision, validation, and writing of the original draft.

ETHIC STATEMENT

The authors declare they have no conflict of interest.

REFERENCES

1. G. Kickelbick, ed. *Hybrid Materials : Synthesis, characterization and apllications*. (Wiley-VCH Verlag GmbH & Co, 2006).

2. C. Sanchez, P. Belleville, M. Popall, and L. Nicole, "Applications of advanced hybrid organic-inorganic nanomaterials: from laboratory to market," *Chem. Soc. Rev.,* **40**(2), 696-753 (2011).

3. L. Nicole, C. Laberty-Robert, L. Rozes, and C. Sanchez, "Hybrid materials science: a promised land for the integrative design of multifunctional materials," *Nanoscale,* **6**(12), 6267-6292 (2014).

4. C. Sanchez, et al., ""“Chimie douce”: A land of opportunities for the designed construction of functional inorganic and hybrid organic-inorganic nanomaterials," *Comptes Rendus Chimie,* **13**(1), 3-39 (2010).

5. A.M. Díez-Pascual, "Nanoparticle Reinforced Polymers," *Polymers,* **11**(4) (2019).

6. C. Sanchez, B. Lebeau, F. Chaput, and J.P. Boilot, "Optical Properties of Functional Hybrid Organic–Inorganic Nanocomposites," *Adv. Mater.,* **15**(23), 1969-1994 (2003).

7. A. Ovsianikov, et al., "Two-photon polymerization of hybrid sol-gel materials for photonics applications," *Laser Chem.,* **2008** (2008).

8. M. Malinauskas, M. Farsari, A. Piskarskas, and S. Juodkazis, "Ultrafast laser nanostructuring of photopolymers: A decade of advances," *Physics Reports,* **533**(1), 1-31 (2013).

9. I. Sakellari, et al., "Two-photon polymerization of titanium-containing sol–gel composites for three-dimensional structure fabrication," *Appl. Phys. A,* **100**(2), 359-364 (2010).

10. E. Andrzejewska, *Chapter 2 - Free Radical Photopolymerization of Multifunctional Monomers*, in *Three-Dimensional Microfabrication Using Two-photon Polymerization*, T. Baldacchini, Editor. 2016, William Andrew Publishing: Oxford. 62-81.

11. D.S. Achilias, "A Review of Modeling of Diffusion Controlled Polymerization Reactions," *Macromol. Theory Simul.,* **16**(4), 319-347 (2007).

12. J.-D. Cho, Y.-B. Kim, H.-T. Ju, and J.-W. Hong, "The effects of silica nanoparticles on the photocuring behaviors of UV-curable polyester acrylate-based coating systems," *Macromolecular Research,* **13**(4), 362-365 (2005).

13. J.-D. Cho, H.-T. Ju, and J.-W. Hong, "Photocuring kinetics of UV-initiated free-radical photopolymerizations with and without silica nanoparticles," *J. Polym. Sci., Part A: Polym. Chem.,* **43**(3), 658-670 (2005).

14. H. Kaddami, J.P. Pascault, and J.F. Gerard, "Influence of the initiation rate on the polymerization kinetics of hydroxy ethyl methacrylate (HEMA) filled with HEMA-grafted silica preformed nanoparticles," *Polymer Engineering & Science,* **44**(7), 1231-1239 (2004).

15. H. Kaddami, J.F. Gerard, P. Hajji, and J.P. Pascault, "Silica-filled poly(HEMA) from hema/grafted SiO2 nanoparticles: Polymerization kinetics and rheological changes," *J. Appl. Polym. Sci.,* **73**(13), 2701-2713 (1999).

16. D. Achilias and P. Siafaka, "Polymerization kinetics of poly (2-Hydroxyethyl methacrylate) hydrogels and Nanocomposite materials," *Processes,* **5**(2), 21 (2017).

17. C. Lin, et al., "Effects of Surface Groups on SiO2 Nanoparticles on in Situ Solution Polymerization: Kinetics and Mechanism," *Industrial & Engineering Chemistry Research,* **57**(45), 15280-15290 (2018).

18. M.M. Demir, M. Memesa, P. Castignolles, and G. Wegner, "PMMA/Zinc Oxide Nanocomposites Prepared by In-Situ Bulk Polymerization," *Macromol. Rapid Commun.,* **27**(10), 763-770 (2006).

19. M. Michailidis, G.D. Verros, E.A. Deliyanni, E.G. Andriotis, and D.S. Achilias, "An experimental and theoretical study of butyl methacrylate in situ radical polymerization kinetics in the presence of graphene oxide nanoadditive," *J. Polym. Sci., Part A: Polym. Chem.,* **55**(8), 1433-1441 (2017).

20. G.D. Verros and D.S. Achilias, "Toward the development of a mathematical model for the bulk in situ radical polymerization of methyl methacrylate in the presence of nano-additives," *The Canadian Journal of Chemical Engineering,* **94**(9), 1783-1791 (2016).

21. S. Parola, B. Julián‐López, L.D. Carlos, and C. Sanchez, "Optical properties of hybrid organic‐inorganic materials and their applications," *Adv. Funct. Mater.,* **26**(36), 6506-6544 (2016).

22. B. Lebeau and P. Innocenzi, "Hybrid materials for optics and photonics," *Chem. Soc. Rev.,* **40**(2), 886-906 (2011).

23. P. Gorbovyi, et al., "Novel nanostructured pHEMA-TiO2 hybrid materials with efficient light-induced charge separation," *Nanoscale,* **3**(4), 1807-1812 (2011).

24. P. Gorbovyi, A. Uklein, M. Traore, L. Museur, and A. Kanaev, "Formation of gel of preformed size-selected titanium-oxo-alkoxy nanoparticles: towards organic-inorganic hybrid material with efficient interfacial electron transfer," *Mater. Res. Express,* **1**(4) (2014).

25. P. Gorbovyi, et al., "Alkoxysilane effect in hybrid material: A comparison of pHEMA-TiO2 and pMAPTMS-TiO2 nanoparticulate hybrids," *Mater. Res. Bull.,* **114**, 130-137 (2019).

26. L. Museur, et al., "Luminescence properties of pHEMA-TiO2 gels based hybrids materials," *J. Lumin.,* **132**(5), 1192-1199 (2012).

27. E. Evlyukhin, et al., "Synthesis of organic–inorganic hybrids via a high-pressure-ramp process: the effect of inorganic nanoparticle loading on structural and photochromic properties," *Nanoscale,* **10**(47), 22293-22301 (2018).

28. E. Evlyukhin, et al., "Laser Assisted High Pressure Induced Polymerization of 2-(hydroxyethyl) Methacrylate," *J. Phys. Chem. B,* **119**(8), 3577-3582 (2015).

29. E. Evlyukhin, et al., "A New Route for High-Purity Organic Materials: High-Pressure-Ramp-Induced Ultrafast Polymerization of 2-(Hydroxyethyl)Methacrylate," *Scientific Reports,* **5**, 18244 (2016).

30. Z. Jia, et al., "Polymerization initiation of pure 2-hydroxyethylmethacrylate under shock wave compression," *New J. Chem.,* **46**(19), 9258-9263 (2022).

31. A.I. Kuznetsov, et al., "Laser-induced photopatterning of organic–inorganic TiO 2-based hybrid materials with tunable interfacial electron transfer," *PCCP,* **11**(8), 1248-1257 (2009).

32. A. Uklein, P. Gorbovyi, M. Traore, L. Museur, and A. Kanaev, "Photo-induced refraction of nanoparticulate organic-inorganic TiO2-pHEMA hybrids," *Opt. Mater. Express,* **3**(5), 533-545 (2013).

33. M. Farsari and B.N. Chichkov, "Materials processing: Two-photon fabrication," *Nat Photon,* **3**(8), 450 (2009).

34. M.T. Do, et al., "Submicrometer 3D structures fabrication enabled by one-photon absorption direct laser writing," *Opt. Express,* **21**(18), 20964-20973 (2013).

35. R. Azouani, et al., "Stability and Growth of Titanium-oxo-alkoxy TixOy(OiPr)z Clusters," *The Journal of Physical Chemistry C,* **111**(44), 16243-16248 (2007).

36. G. Odian, *Principles of polymerization*. 2004: John Wiley & Sons.

37. M. Lang, S. Hirner, F. Wiesbrock, and P. Fuchs, "A Review on Modeling Cure Kinetics and Mechanisms of Photopolymerization," *Polymers,* **14**(10), 2074 (2022).

38. T.T.H. Luu, Z. Jia, A. Kanaev, and L. Museur, "Effect of Light Intensity on the Free-Radical Photopolymerization Kinetics of 2-Hydroxyethyl Methacrylate: Experiments and Simulations," *J. Phys. Chem. B,* **124**(31), 6857-6866 (2020).

39. E. Andrzejewska, "Photopolymerization kinetics of multifunctional monomers," *Prog. Polym. Sci.,* **26**(4), 605-665 (2001).

40. I.S. Tsagkalias and D.S. Achilias, "Role of Functional Groups in the Monomer Molecule on the Radical Polymerization in the Presence of Graphene Oxide. Polymerization of Hydroxyethyl Acrylate under Isothermal and Non-Isothermal Conditions," *Molecules,* **27**(2), 345 (2022).

41. M.D. Goodner, H.R. Lee, and C.N. Bowman, "Method for Determining the Kinetic Parameters in Diffusion-Controlled Free-Radical Homopolymerizations," *Industrial & Engineering Chemistry Research,* **36**(4), 1247-1252 (1997).

42. S. Jockusch, et al., "A steady-state and picosecond pump-probe investigation of the photophysics of an acyl and a bis (acyl) phosphine oxide," *J. Am. Chem. Soc.,* **119**(47), 11495-11501 (1997).

43. S. Morita, "Hydrogen-bonds structure in poly(2-hydroxyethyl methacrylate) studied by temperature-dependent infrared spectroscopy," *Frontiers in Chemistry,* **2**(10) (2014).

44. S. Morita, K. Kitagawa, and Y. Ozaki, "Hydrogen-bond structures in poly(2-hydroxyethyl methacrylate): Infrared spectroscopy and quantum chemical calculations with model compounds," *Vib. Spectrosc,* **51**(1), 28-33 (2009).

45. Z. Jia, et al., "Growth of Silver Nanoclusters on Monolayer Nanoparticulate Titanium-oxo-alkoxy Coatings," *The Journal of Physical Chemistry C,* **116**(32), 17239-17247 (2012).